

Draft: Tuesday 7th August, 2018-10:58

IHEP-CEPC-DR-2018-XX

IHEP-EP-2018-XX

IHEP-TH-2018-XX

CEPC

Conceptual Design Report

Volume II - Physics & Detector

The CEPC Study Group

Fall 2018

Draft: Tuesday 7th August, 2018-10:58

Draft-V0.5

ACKNOWLEDGMENTS

The CEPC Physics and Detector Conceptual Design Report (CDR) was prepared and written by the CEPC Study Group. The study was organised and led by scientists from the Institute of High Energy Physics (IHEP) of the Chinese Academy of Sciences (CAS), and from many universities and other institutes in China and abroad. The study was partially supported ...

...

Draft: Tuesday 7th August, 2018-10:58

Draft-V0.5

CONTENTS

Acknowledgments	iii
1 Benchmark Physics	1
1.1 W and Z Boson Physics	3
1.1.1 Z pole measurements	3
1.1.2 Measurement of the W boson mass	8
1.1.3 Oblique Parameter	12

Draft: Tuesday 7th August, 2018-10:58

Draft-V0.5

CHAPTER 1

BENCHMARK PHYSICS

The historic discovery of a Higgs boson in 2012 by the ATLAS and CMS collaborations [1, 2] and the subsequent studies of the properties of the particle [3–9] indicate the compatibility with the Standard Model (SM) predictions. Although all of the particles in the SM have been discovered, some fundamental questions, e.g. vast difference between the Planck scale and the weak scale, the nature of electroweak phase transition have not been fully understood. The attempt to further address those questions will involve the new physics beyond the SM which could lead a deviation from SM expectations for the precision measurement of the SM. A circular electron positron collider will provide an unique opportunity to have precise measurements of the Higgs, W and Z properties.

The CEPC produces huge statistics of massive SM Bosons. Its physics potential is explored on two different classes of physics benchmarks, the Higgs physics, the precision EW physics. Using the software tools introduced in section ??, the physics potential on Higgs physics is analyzed at full simulation level, see section ?. The accuracies on the EW precision measurements are mainly limited by systematic errors and are estimated in section 1.1. The synergies of these different physics measurements, the complimentary and comparison to the HL-LHC and other high energy physics programs are discussed in Chapter ??.

References

- [1] ATLAS Collaboration Collaboration, *Observation of a new particle in the search for the Standard Model Higgs boson with the ATLAS detector at the LHC*, *Phys. Lett. B* **716** (2012) 1, [arXiv:1207.7214 \[hep-ex\]](#).
- [2] CMS Collaboration Collaboration, *Observation of a new boson at a mass of 125 GeV*

with the CMS experiment at the LHC, *Phys. Lett.* **B716** (2012) 30, [arXiv:1207.7235 \[hep-ex\]](#).

- [3] ATLAS Collaboration, G. Aad et al., *Measurements of Higgs boson production and couplings in diboson final states with the ATLAS detector at the LHC*, *Phys. Lett.* **B726** (2013) 88–119, [arXiv:1307.1427 \[hep-ex\]](#). [Erratum: *Phys. Lett.* **B734**, 406(2014)].
- [4] ATLAS Collaboration, G. Aad et al., *Evidence for the spin-0 nature of the Higgs boson using ATLAS data*, *Phys. Lett.* **B726** (2013) 120–144, [arXiv:1307.1432 \[hep-ex\]](#).
- [5] CMS Collaboration Collaboration, S. Chatrchyan et al., *Observation of a new boson with mass near 125 GeV in pp collisions at $\sqrt{s} = 7$ and 8 TeV*, *JHEP* **1306** (2013) 081, [arXiv:1303.4571 \[hep-ex\]](#).
- [6] CMS Collaboration Collaboration, *Evidence for the direct decay of the 125 GeV Higgs boson to fermions*, *Nature Phys.* **10** (2014), [arXiv:1401.6527 \[hep-ex\]](#).
- [7] CMS Collaboration, V. Khachatryan et al., *Constraints on the spin-parity and anomalous HVV couplings of the Higgs boson in proton collisions at 7 and 8 TeV*, *Phys. Rev.* **D92** (2015) no. 1, 012004, [arXiv:1411.3441 \[hep-ex\]](#).
- [8] ATLAS, CMS Collaboration, G. Aad et al., *Combined Measurement of the Higgs Boson Mass in pp Collisions at $\sqrt{s} = 7$ and 8 TeV with the ATLAS and CMS Experiments*, *Phys. Rev. Lett.* **114** (2015) 191803, [arXiv:1503.07589 \[hep-ex\]](#).
- [9] ATLAS, CMS Collaboration, G. Aad et al., *Measurements of the Higgs boson production and decay rates and constraints on its couplings from a combined ATLAS and CMS analysis of the LHC pp collision data at $\sqrt{s} = 7$ and 8 TeV*, *JHEP* **08** (2016) 045, [arXiv:1606.02266 \[hep-ex\]](#).

1.1 W and Z Boson Physics

With high production cross sections and large integrated luminosity, the CEPC will reach a new level of precision for the measurements of the properties of the W and Z bosons. Precise measurements of the W and Z boson masses, widths, and couplings are critical to test the consistency of the SM [1]. In addition, many BSM models predict new couplings of the W and Z bosons to other elementary particles. Precise electroweak measurements performed at the CEPC could discover deviations from the SM predictions and reveal the existence of new particles that are beyond the reaches of direct searches at the current experiments.

Significant improvements are expected from the CEPC measurements. Table 1.1 lists the expected precision from CEPC compared to achieved precisions from the LEP experiments for various measurements. Details about the estimation of these uncertainties are described in this section.

Table 1.1: The expected precision in a selected set of EW precision measurements in CEPC and the comparison with the precision from LEP experiments. The CEPC accelerator running mode and total integrated luminosity expected for each measurement are also listed. Depending on detector solenoid field during Z pole operation, the integrated luminosity varied from 8 ab^{-1} to 16 ab^{-1} .

Observable	LEP precision	CEPC precision	CEPC runs	$\int \mathcal{L}$ needed in CEPC
m_Z	2 MeV	0.5 MeV	Z threshold scan	$8\text{--}16 \text{ ab}^{-1}$
$A_{FB}^{0,b}$	1.7%	0.1%	Z threshold scan	$8\text{--}16 \text{ ab}^{-1}$
$A_{FB}^{0,\mu}$	7.7%	0.3%	Z threshold scan	$8\text{--}16 \text{ ab}^{-1}$
$A_{FB}^{0,e}$	17%	0.5%	Z threshold scan	$8\text{--}16 \text{ ab}^{-1}$
$\sin^2 \theta_W^{\text{eff}}$	0.07%	0.001%	Z threshold scan	$8\text{--}16 \text{ ab}^{-1}$
R_b	0.3%	0.02%	Z pole	$8\text{--}16 \text{ ab}^{-1}$
R_μ	0.2%	0.01%	Z pole	$8\text{--}16 \text{ ab}^{-1}$
N_ν	1.7%	0.05%	ZH runs	5.6 ab^{-1}
m_W	33 MeV	2-3 MeV	ZH runs	5.6 ab^{-1}
m_W	33 MeV	1 MeV	WW threshold	2.6 ab^{-1}

1.1.1 Z pole measurements

The CEPC offers the possibility of dedicated low-energy runs at the Z pole for at least two years with a high instantaneous luminosity ($1.6 - 3.2 \times 10^{35} \text{ cm}^{-2} \text{ s}^{-1}$). The expected integrated luminosity for CEPC Z pole runs is more than 8 ab^{-1} , and it is expected to produce about 10^{12} Z bosons (Tera- Z).

These runs allow high precision electroweak measurements of the Z boson decay partial widths, e.g. the parameters $R_b = \Gamma_{Z \rightarrow b\bar{b}}/\Gamma_{\text{had}}$ and $R_\ell = \Gamma_{\text{had}}/\Gamma_{Z \rightarrow \ell\bar{\ell}}$ ¹. It would also perform high precision measurements of the forward-backward charge asymmetry (A_{FB}), the effective weak mixing angle ($\sin^2 \theta_W^{\text{eff}}$), number of light neutrino species (N_ν), and the mass of the Z boson (M_Z). It is also possible to perform some measurements with the Z boson without these dedicated low-energy runs near or at the Z pole. For example, the direct measurement of the number of light neutrino species can be performed in ZH runs at 240 GeV.

1.1.1.1 R_b

The partial width of the Z boson to its individual decay channel is proportional to the square of the fundamental Z -fermion couplings. The ratio of the partial widths R_b is sensitive to electroweak radiative corrections from new particles. For example, the existence of the scalar top quarks or charginos in supersymmetry could lead to a visible change of R_b from the SM prediction.

Precise measurements of R_b have been made by LEP collaborations [2–6] and by the SLD collaboration [7] using hadronic Z events.

Decays of b -hadrons were tagged using tracks with large impact parameters and/or reconstructed secondary vertices, complemented by event shape variables. The combination of LEP and SLD measurements yields a value of 0.21629 ± 0.00066 for R_b . The relative statistical uncertainty of R_b is above 0.2%, and systematic uncertainty is about 0.2%.

A relative precision of 0.05% can be achieved for the measurement of R_b at the CEPC, and it will improve the current precision in experimental measurement by one order of magnitude. The statistical uncertainty improves by two order of magnitude and the systematic uncertainties will also reduce. **the above two sentences are confusing.** The main systematic uncertainty is due to hemisphere tag correlations in $Z \rightarrow b\bar{b}$ events (0.05%). The uncertainty due to hemisphere tag correlations can be reduced to a level of 0.05% from the expected improvement in the b -tagging performance of the CEPC detector. The improvement of b -tagging efficiency is important to reduce this correlation which becomes irrelevant in the limit of 100% b -tagging efficiency. Due to that fact that a next-generation vertex detector will be used in the CEPC detector, the b -tagging efficiency is expected to be around 70% with a b -jet purity of 95% as shown in Fig. ??, which is about 15%-20% higher than the efficiency achieved in previous experiments. The uncertainty due to hemisphere tag correlations can be reduce to 0.05% level, which is a factor of four lower than previous measurements.

1.1.1.2 The partial decay width of $Z \rightarrow \mu^+\mu^-$

The $\mu^+\mu^-$ channel provides the cleanest leptonic final state. Combining the measurements from all four LEP experiments [8–11], the overall uncertainty of R_μ is 0.2%. The statistical uncertainty of R_μ is 0.15%.

A precision of 0.01% can be achieved at the CEPC. The main systematic is the uncertainty of photon energy scale in the $Z \rightarrow \mu^+\mu^-\gamma$ process. About 2% of the $Z \rightarrow \mu^+\mu^-$ sample are classified as $Z \rightarrow \mu^+\mu^-\gamma$ events with a photon detected in ECAL. For this class of events, the most critical cut is that on the difference between the expected and

¹Here R_ℓ is defined as the ratio to any *one* charged lepton flavor, assuming lepton universality, not the ratio to the sum of all lepton flavors.

measured photon energy ($|E_{\gamma}^{expected} - E_{\gamma}^{measured}| < 5\sigma_{\gamma}$), which is very efficient in removing the $Z \rightarrow \tau\tau$ background. The

The energy resolution in the EM calorimeter of the CEPC detector is expected to be $16\%/\sqrt{E}$, which is significantly better than the resolution in previous measurements. Therefore, the uncertainty due to photon energy scale and resolution in $Z \rightarrow \mu^+\mu^-\gamma$ process can be reduced to 0.01%. The main challenge in this measurement is to reduce the systematics due to QED ISR events. More detailed studies of radiative events in Z threshold scan runs are expected. Benefitting from high statistics in Z threshold scan runs, the source of uncertainty can be reduced to a level of 0.03%.

1.1.1.3 The forward-backward asymmetry A_{FB}^b at the Z pole

The measurement of the forward-backward asymmetry in $e^+e^- \rightarrow b\bar{b}$ events at the Z pole, $A_{FB}^{b,0}$, gives an important test of the Standard Model. $A_{FB}^{b,0}$ offers the most precise determination of the weak mixing angle. The measurements have been made at SLD and LEP experiments [12–16].

$Z \rightarrow b\bar{b}$ events were identified by tagging two b jets. Each event was divided into forward and backward categories by the plane perpendicular to the thrust axis which contains the interaction point. The combination of the LEP and SLD measurements gives a measured value of $A_{FB}^{b,0} = 0.1000 \pm 0.0017$. The statistical uncertainty is 1.2% and the main systematic uncertainties come from hemisphere tag correlations for b events (1.2%), tracking resolution and vertex detector alignment (0.8%), charm physics modeling (0.5%), and QCD and thrust axis correction (0.7%).

A precision of 10^{-4} can be achieved for the measurement of $A_{FB}^{b,0}$ at the CEPC, improving the current precision by more than a factor of 10. The expected statistical uncertainty is at a level of 0.05%. The uncertainty due to hemisphere tag correlations for b events can be reduced to 0.1% due to high b -tagging efficiency. The uncertainty due to charm physics modeling can be reduced to 0.05% by choosing a tighter b -tagging working point. The uncertainty due to tracking resolution and vertex detector alignment can be reduced to 0.05%. The expected tracking momentum resolution in the CEPC detector is $\sigma/p_T = 2 \times 10^{-4} \times p_T + 0.005$, which is 10 times better than the resolutions of the LEP detectors. The uncertainty due to QCD and thrust axis correction can be reduced to 0.1% due to at least 10 times better granularity in the CEPC calorimeters. Overall, the expected systematics at CEPC measurement can be reduced to a level of 0.15%.

1.1.1.4 The prospects for the effective weak mixing angle measurement

The weak mixing angle $\sin^2 \theta_W^{\text{eff}}$ is a very important parameter in the electroweak theory of the SM. It is the only free parameter that fixes the relative couplings of all fermions to the Z . It describes the rotation of the original W^0 and B^0 vector boson states into the observed γ and Z bosons as a result of spontaneous symmetry breaking. The weak mixing angle is very sensitive to electroweak radiative corrections, and it can be used to perform a precise test of the SM theory. Furthermore, if there is any new heavy gauge boson Z' , the weak mixing angle is expected to deviate from the SM prediction due to the contribution from physics in loop corrections. Therefore $\sin^2 \theta_W^{\text{eff}}$ is very sensitive to new physics as well.

The centre-of-mass energy dependence of the forward-backward asymmetry arises from the interference of the Z boson with the virtual photon and thus depends on $\sin^2 \theta_W^{\text{eff}}$. In

other words, the effective weak mixing angle can be extracted by studying the \sqrt{s} dependence of the forward-backward asymmetry.

The effective weak mixing angle measurement has been performed in LEP using $Z \rightarrow b\bar{b}$ events and $Z \rightarrow \ell^+\ell^-$ events. The forward-backward asymmetry A_{FB} in one Z -pole dataset and two off Z -pole datasets ($\sqrt{s} = 89.4$ GeV, $\sqrt{s} = 93.0$ GeV) are used to extract $\sin^2 \theta_W^{\text{eff}}$. The current experimental result is $\sin^2 \theta_W^{\text{eff}} = 0.23153 \pm 0.00016$. $Z \rightarrow b\bar{b}$ events were identified by tagging two b jets. The main uncertainty includes uncertainty on the A_{FB}^b measurement as described in Sec. 1.1.1.3. and the statistical uncertainty in off Z -pole datasets.

Both Z -pole and off Z -pole runs are needed to perform the effective weak mixing angle measurement at the CEPC. The Z off-peak runs are expensive, therefore we need to optimize the integrated luminosity for off-peak runs. In order to improve the precision of $\sin^2 \theta_W^{\text{eff}}$ by a factor of 3, the required CEPC integrated luminosity for Z -pole runs are $8 - 16 \text{ ab}^{-1}$ and at least $2 - 4 \text{ ab}^{-1}$ integrated luminosity is needed for off Z -pole runs. The expected precision of effective weak mixing angle measurement in CEPC using $Z \rightarrow b\bar{b}$ events is expected to be 0.02%.

1.1.1.5 Z mass measurement

The mass m_Z is a fundamental parameter in the SM and was determined with an overall uncertainty of 2 MeV by four LEP experiments. The mass scan around the Z peak was performed from 88 GeV to 94 GeV. The Z mass was measured by a combined fit to the hadronic and leptonic cross sections in the on-peak and off-peak datasets. Most of the m_Z information is extracted from the off-peak runs. Taking the OPAL measurement as one example, six off-peak datasets were used to complete the m_Z scan. The main uncertainty of m_Z includes the statistical uncertainty ($1 \text{ MeV}/c^2$), and the LEP beam energy (about $1 \text{ MeV}/c^2$).

A precision of 0.5 MeV can be achieved in CEPC measurement. The mass scan around the Z peak is the key for improving m_Z measurements.

The LEP measurement was limited by the statistics in their off-peak runs, therefore the luminosity in Z off-peak runs plays an important role in the m_Z measurement. We propose six off-peak runs and one on-peak run in CEPC Z mass scan, as listed in Table ???. The expected m_Z uncertainty in CEPC due to statistics is about 0.1 MeV.

Another important systematic is beam momentum scale uncertainty. The beam momentum uncertainty in the CEPC accelerator is expected to be accurate to the 10 ppm level, which is about five times better than LEP. The uncertainty on m_Z due to the uncertainty on the beam energy can be reduced to less than 0.5 MeV.

Hadronic decay channels of the Z events are also expected to be used to measure m_Z since the leptonic decay channels suffer from low statistics. The uncertainty due to jet energy scale and resolution results in about 0.1 MeV in the m_Z measurement.

1.1.1.6 Neutrino species counting

Two different methods have been used to determine the number of neutrino species (N_ν) at LEP.

The first method is an indirect method using the analysis of the Z lineshape, and it uses the data collected by the Z threshold scan runs. The second method is a direct measurement, which is based on the measurement of the cross section for the radiative process $e^+e^- \rightarrow \nu\nu\gamma$. The second method at CEPC is supposed to use the ZH runs.

These two methods use different theoretical inputs from the Standard Model and also use completely different datasets, therefore they are independent and complementary. The sensitivity to new physics will be different for these two methods. In the direct method, one can measure N_ν as a function of *sqrts*. This is very sensitive to new physics at high energy scales. Possible contributions include WIMP dark matter particles, and other weakly coupled particles such as exotic neutrinos, gravitinos, or KK gravitons in theories with large extra dimensions. Thus, when we refer to the number of neutrino species, we actually include any number of possible invisible particles other than neutrinos.

Indirect method from Z line shape The indirect method assumed all contributions from invisible channels are coming from the $Z \rightarrow \nu\bar{\nu}$. This method used the analysis of Z line-shape, subtracting the visible partial widths of the hadrons (Γ_{had}), and the partial widths of the leptons (Γ_ℓ) from the total width Γ_Z . The invisible width Γ_{inv} can be written as:

$$\Gamma_{\text{inv}} = N_\nu \Gamma_\nu = \Gamma_Z - \Gamma_{\text{had}} - 3\Gamma_\ell. \quad (1.1)$$

We take as our definition of the number of neutrinos $N_\nu = \Gamma_{\text{inv}}/\Gamma_\nu$, i.e. the ratio of the invisible width to the Standard Model expectation for the partial width to a single neutrino species.

Using the input from SM model, we can rewrite equation 1.1 as the following:

$$N_\nu = \frac{\Gamma_\ell}{\Gamma_\nu} \left(\sqrt{\frac{12\pi R_\ell}{M_Z^2 \sigma_{\text{had}}^0}} - R_\ell - 3 \right). \quad (1.2)$$

As shown in equation 1.2, the precision of N_ν depends on the the lepton partial width R_ℓ measurement, the Z mass measurement, and the hadronic cross section of the Z boson on its mass peak (σ_{had}^0). The precision of σ_{had}^0 gives the largest impact to N_ν measurement, and it is very sensitive to the precision of the luminosity. Therefore the precise luminosity measurement is the key to determine N_ν .

Precise measurements of N_ν have been made by LEP collaborations, and they obtained a precision of 0.27% using this indirect method. The main systematics of the N_ν measurement is coming from the uncertainty of luminosity (0.14%) and the theory uncertainty in the predicted cross section of the small angle Bhabha process (0.11%).

The precision of 0.1% in N_ν measurement with the indirect method can be achieved in CEPC measurement, which improves the current precision by a factor of three. Benefitting from the recent development of luminosity detector technology, the uncertainty due to luminosity can be reduced to 0.05%. The uncertainty from the small angle Bhabha process can be reduced to 0.05% due to recent progress in studying this process.

Direct method using $e^+e^- \rightarrow \nu\bar{\nu}\gamma$ events The most precise direct N_ν measurements at LEP were carried out by the L3 collaboration and Delphi collaboration. By combining the direct measurements at LEP, the current experimental result is $N_\nu = 2.92 \pm 0.05$. The statistical uncertainty of N_ν in the previous measurement is 1.7%. The main systematic uncertainty from the L3 measurement includes the uncertainty in single photon trigger efficiency (0.6%), and photon identification efficiency (0.3%), and the uncertainty in identifying the converted photons (0.5%).

A precision of 0.2% can be achieved for the direct measurement of N_ν at CEPC, and it will improve the current precision by a factor of 10. Due to the excellent performance

of the CEPC inner tracker, the uncertainty due to converted photons' selection efficiency is expected to be negligible. The granularity of the CEPC EM calorimeter is expected to be 10 to 100 times better than the detectors at LEP. Therefore photons can be identified with high purity with loose EM shower shape based selection. The uncertainty of photon efficiency can be reduced to less than 0.05%.

1.1.2 Measurement of the W boson mass

In e^+e^- collisions, W bosons are mainly produced in pairs, through the reaction $e^+e^- \rightarrow W^+W^-$. At threshold, $\sqrt{s} \sim 2m_W$, the cross section of this process is very sensitive to m_W , providing a natural method for the measurement of this parameter. At centre-of-mass energies above the W^+W^- production threshold, m_W can be determined from the peak of the invariant mass distribution of its decay products. Both methods are very complementary : while the former requires an accurate theoretical prediction of the W^+W^- production cross section as a function of m_W and a precise determination of the collider luminosity, the latter mostly relies on a good resolution in the reconstruction of the hadronic invariant mass, and a precise control of the detector calibration.

Both methods have been used at LEP. With only about 40 pb^{-1} collected by the four LEP experiments at $\sqrt{s} \sim 161.3 \text{ GeV}$ and given the low cross section at threshold, the former is limited by a significant statistical uncertainty of about 200 MeV. The final state reconstruction method exploited the full LEP2 dataset, about 2.6 fb^{-1} collected between $\sqrt{s} \sim 161.3 \text{ GeV}$ and 206 GeV, and achieved a total uncertainty of 33 MeV. While this measurement used both the $W^+W^- \rightarrow \ell\nu qq$ and $W^+W^- \rightarrow qq qq$ channels, the fully hadronic channel is limited by uncertainties in the modeling of hadronization and interactions between the decaying W bosons, and the semi-leptonic final state dominates the precision of the final result.

Accounting for results from the CDF and D0 experiments at the TeVatron, and from ATLAS at the LHC, the present world-average value of m_W has an uncertainty estimated between 12 and 13 MeV. The uncertainty is expected to fall below 10 MeV when including final LHC measurement results. A natural goal for CEPC is thus to reach a precision well below 5 MeV, making optimal use of W^+W^- cross section data around $\sqrt{s} \sim 161 \text{ GeV}$, and of the final state invariant mass distributions at $\sqrt{s} \sim 240 \text{ GeV}$. The achievable precision of both methods is described below.

Determination of m_W and Γ_W from the W^+W^- production cross section

In this section, the possibility of extracting the W boson mass and width from the production cross section is explored. The study assumes a total integrated luminosity of $L = 3.2 \text{ ab}^{-1}$, which can be collected in **XYZ years**, assuming an instantaneous luminosity of **XYZ**. For this study, the GENTLE program version 2.0 [] is used to calculate $\sigma_{W^+W^-}$ as a function of the centre-of-mass energy, m_W and Γ_W . The behaviour of the cross section as a function of the centre-of-mass energy, $E_{\text{c.m.}}$, is illustrated in Figure 1.1.

The statistical sensitivity of the measurement is optimized in the following way:

- the total integrated luminosity is shared between one, two or three values of $E_{\text{c.m.}}$;
- in the two-point scenario, a three-dimensional optimization is performed, scanning both values $E_{\text{c.m.}}$ in steps of 100 MeV, and the fraction of integrated luminosity spent at each point in steps of 5%;

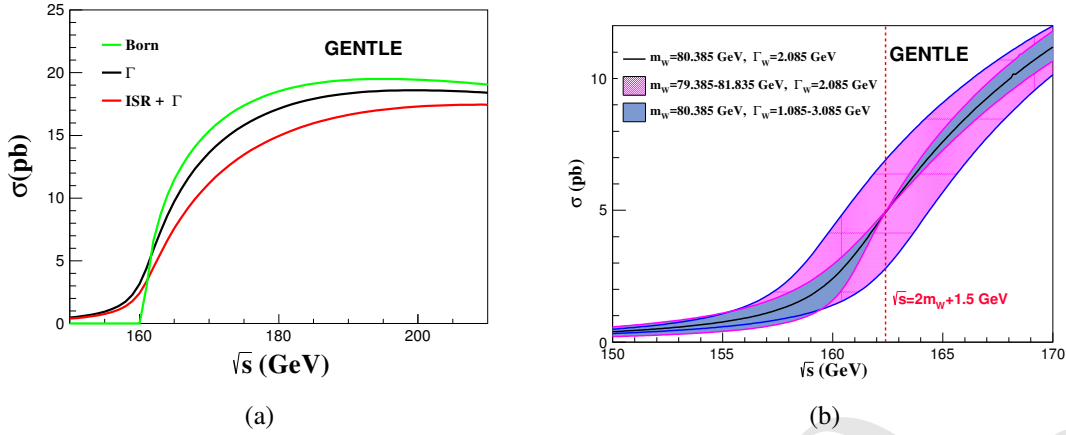


Figure 1.1: W^+W^- production as a function of $E_{c.m.}$, (a) at Born level, including finite width effects, and including initial state radiation corrections; and (b) for a range of values of m_W and Γ_W .

- in the three point scenario, a corresponding five-dimensional optimization is performed.

Sources of systematic uncertainties can be categorized as correlated or uncorrelated between measurements at different values of $E_{c.m.}$. The following sources are considered:

- **Uncorrelated sources:** this category includes the uncertainties associated with the beam energy calibration, and the beam energy spread. For the former, an uncertainty of 0.5 MeV is assumed, and the latter can be controlled to 1%, at each value of $E_{c.m.}$;
- **Correlated sources:** this category includes the uncertainties from the integrated luminosity, the detection efficiency, the purity, and the theoretical W-pair cross section. It is assumed that these sources sum up to a total relative uncertainty of 2×10^{-4} on the ratio between measured and predicted cross sections.

The result of the statistical optimization leads to a three-point scenario, with most of the data collected at energies of 157.5 and 162.5 GeV. A summary of given in Table 1.2. The final measurement uncertainties, assuming this optimal scenario and systematic uncertainties are described above, are collected in Table 1.3. We conclude that an uncertainty of about 1 MeV can be achieved for m_W , and 3 MeV for Γ_W . While the former is still dominated by statistical uncertainties, the latter is significantly affected by the beam energy spread.

Determination of m_W by kinematic reconstruction

According to LEP experience, the fully hadronic final state is limited by systematic uncertainties that are difficult to control using data. The present section therefore concentrates on the semi-leptonic final states, where one W boson decays to an electron or a muon, while the other decays hadronically. An estimate of the m_W measurement potential is presented based on $WW \rightarrow \ell\nu qq$ events ($\ell = e, \mu$), and the potential of hadronic Z boson decays to calibrate the measurement of the hadronic invariant mass is evaluated.

The W^+W^- cross section at $\sqrt{s} = 240$ GeV is about 17 pb. For an integrated luminosity of 5.6 ab^{-1} , this corresponds to a sample of about 95×10^6 W boson pairs, and 28×10^6 $WW \rightarrow \ell\nu qq$ events. For ZZ production, the cross section is about 1 pb, yielding about

Table 1.2: The proposed 3 $e^+e^- \rightarrow W^+W^-$ threshold scan runs and their integrated luminosity, for a total integrated luminosity of 3.2 ab^{-1} .

Beam Energy (GeV)	Luminosity (ab^{-1})
157.5	1.0
161.5	0.2
162.5	2.0

Table 1.3: Dominant systematic uncertainties in the measurement of m_W and Γ_w , using the production cross section at threshold at CEPC. All numbers are given in MeV.

Observable	m_W	Γ_W
Sources or uncertainty (MeV)		
Statistics	0.8	1.1
Beam energy	0.4	0.5
Beam spread	–	0.9
Corr. syst.	0.5	0.1
Total	1.0	2.9

Table 1.4: Efficiency of the event selection criteria in the $WW \rightarrow \mu\nu qq$ channel.

Selection	Efficiency (%)	Nb. of events
$E_\mu > 10 \text{ GeV}, \cos(\theta_\mu) < 0.995$	85.4	11.9×10^6
$p_T^{\text{miss}} > 10 \text{ GeV}$	82.0	11.5×10^6
$m_{\text{vis}} > 0.5 \times \sqrt{s}$	75.6	10.6×10^6
$b\text{-tag score} < 0.5$	71.3	10.0×10^6

Table 1.5: Efficiency of the event selection criteria in the $ZZ \rightarrow \nu\nu qq$ channel.

Selection	Efficiency (%)	Nb. of events
$E_\mu > 10 \text{ GeV}, \cos(\theta_\mu) < 0.995$		
$m_{\text{vis}} > 0.8 \times \sqrt{s}$		
$b\text{-tag score} < 0.5$		

5.6×10^6 Z boson pairs, and 1.6×10^6 $ZZ \rightarrow \nu\nu qq$ events. While the Z boson mass is more precisely known than m_W and the $Z \rightarrow qq$ resonance provides a useful check of the detector calibration, the sample is small compared to the $W \rightarrow qq$ one, and the presence of heavy quarks in Z boson decays has to be accounted for when deriving constraints on the hadronic response in W events.

W^+W^- event selection criteria will require the presence of one reconstructed electron or muon with energy greater than 10 GeV, and missing transverse momentum greater than 10 GeV. The invariant mass of all reconstructed final state particles should exceed 50% of the centre-of-mass energy; the hadronic system, *i.e.* the set of all particles excluding the selected lepton, is clustered into two jets and its invariant mass distribution is used to probe the W boson mass. A b -tag veto can be applied to enrich the selected samples in light-quark decays, and reduce the systematic differences between the W and Z boson samples. In the $\mu\nu qq$ channel, the efficiency of these criteria is 71.3%, as shown in Table 1.4. Corresponding selection efficiencies for $ZZ \rightarrow \nu\nu qq$ events are shown in Table 1.5. The corresponding hadronic invariant mass distributions are shown in Figure 1.2. After these selections, backgrounds are expected to be small and play a negligible role in the measurement.

Given the large expected statistics, the availability of the $e\nu qq$ channel and the good resolution in the invariant mass distribution, the statistical sensitivity of the m_W measurement is better than 1 MeV. Using the $ZZ \rightarrow \nu\nu qq$ sample alone, the detector calibration can be checked to about 6 MeV. Further calibration samples can be extracted from radiative return events ($e^+e^- \rightarrow Z\gamma$). In addition, runs at $\sqrt{s} = 91.2 \text{ GeV}$ will be required for general detector alignment, monitoring and calibrations; these runs will provide copious samples of hadronic Z boson decays that will further constrain the hadronic calibration. Combining all information, the statistical precision of the calibration samples will match that of the W boson decays.

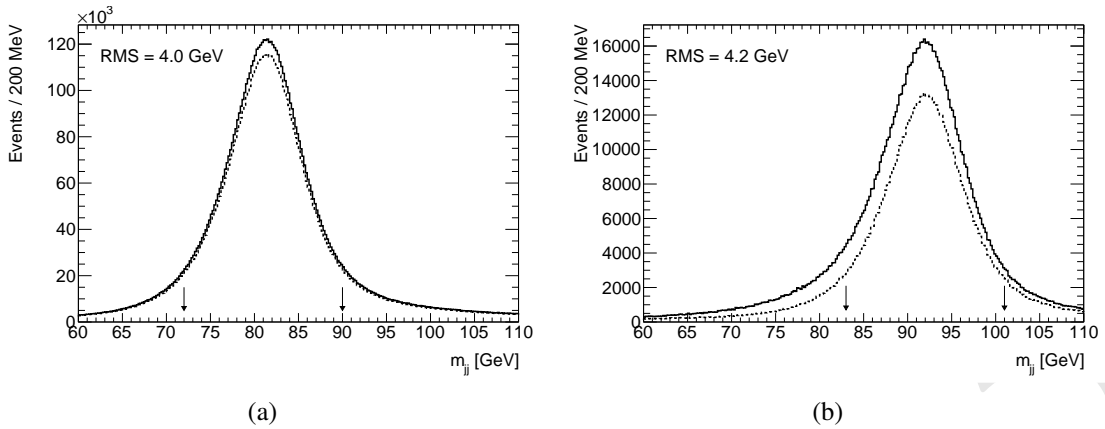


Figure 1.2: Dijet invariant mass distributions for (a) $WW \rightarrow \mu\nu qq$ events, without and with a b -jet veto cut, and correspondingly for (b) $ZZ \rightarrow \nu\nu qq$ events. The RMS of the distributions are quoted for the interval indicated by the arrows.

The statistical sensitivity can be further enhanced using kinematics fits, constraining the reconstructed lepton and jet momenta to match the known center of mass energy ($\sum_i E_i = \sqrt{s}$) and total event momentum ($\sum_i \vec{p}_i = \vec{0}$). This method was routinely used at LEP, gaining a factor of about 3 in the statistical precision, at the expense of an explicit dependence of the measurement on the beam energy. Given the expected statistical precision at CEPC, this refinement seems unnecessary here. In these conditions, the beam energy calibration, and initial state radiation are expected to contribute less than 1 MeV to the measurement uncertainty. Further significant sources of systematic uncertainty include the lepton momentum scale, which can be reduced using Z boson decays as discussed above, and the modelling of hadronization. The latter can be strongly reduced using measurements of rates and distributions of identified particles, in both Z and W boson decays.

The primary sources of uncertainty are summarized in Table 1.6, comparing LEP and CEPC. A total uncertainty at the level of 3 MeV seems reachable.

1.1.3 Oblique Parameter

Using the estimated experimental capabilities of CEPC, we carry out a fit to determine the sensitivity of CEPC to the oblique electroweak parameters S and T [17, 18]. We omit the parameter U that is often included in fits as it arises from a dimension-8 operator in theories with a weakly coupled Higgs boson [19], and so is expected to be much smaller than S and T which arise at dimension 6. In the electroweak fit we treat the following five well-measured observables as parameters, from which the Standard Model prediction for all of the other observables may be computed:

$$\alpha_s(m_Z^2), \Delta\alpha_{\text{had}}^{(5)}(m_Z^2), m_Z, m_t, m_h. \quad (1.3)$$

Of these parameters, CEPC is expected to significantly improve our knowledge of m_Z . The primary power of CEPC is in improving the precision of measurements of other observables, including m_W and $\sin^2 \theta_{\text{eff}}^\ell$, which may be derived from these parameters. Readers interested in more background information may find a thorough and up-to-date review of the status of electroweak precision in Ref. [20].

Table 1.6: Dominant systematic uncertainties in the measurement of m_W using direct reconstruction, as achieved at LEP, and expected at CEPC.

Collider	LEP	CEPC
\sqrt{s} (GeV)	180–203	240
$\int \mathcal{L}$	2.6 fb ⁻¹	5.6 ab ⁻¹
Channels	$\ell\nu qq, qq qq$	$\ell\nu qq$
Sources or uncertainty (MeV)		
Statistics	25	1.0
Beam energy	9	1.0
Hadronization	13	1.5
Radiative corrections	8	1.0
Detector effects	10	1.5
Total	33	3.0

Obs.	Value	Exp. Uncertainty	Th. Uncertainty
$\alpha_s(M_Z^2)$	0.1185	1.0×10^{-4} [21]	1.5×10^{-4}
$\Delta\alpha_{\text{had}}^{(5)}(m_Z^2)$	276.5×10^{-4}	4.7×10^{-5} [22]	–
m_Z [GeV]	91.1875	0.0005	–
m_t [GeV] (pole)	173.34	0.6 [23]	0.25 [24]
m_h [GeV]	125.14	0.1 [22]	–
m_W [GeV]	80.358617 [25]	0.001	1.4×10^{-3}
$A_{\text{FB}}^{0,b}$	0.102971 [26, 27]	1.0×10^{-4}	8.3×10^{-5}
$A_{\text{FB}}^{0,\mu}$	0.016181 [26]	4.9×10^{-5}	2.6×10^{-5}
$A_{\text{FB}}^{0,e}$	0.016181 [26]	8.1×10^{-5}	2.6×10^{-5}
Γ_Z [GeV]	2.494682 [28]	0.0005	2×10^{-4}
$R_b \equiv \Gamma_b/\Gamma_{\text{had}}$	0.2158459 [28]	4.3×10^{-5}	7×10^{-5}
$R_\ell \equiv \Gamma_{\text{had}}/\Gamma_\ell$	20.751285 [28]	2.1×10^{-3}	1.5×10^{-3}
$\Gamma_{Z \rightarrow \text{inv}}$ [GeV]	0.167177 [28]	8.4×10^{-5}	–

Table 1.7: Inputs to the CEPC fit. Numbers in bold are expected experimental uncertainties from CEPC measurements. Other entries reflect anticipated uncertainties at the time of CEPC operation. The numbers in the “Value” column for the first five parameters are current measurements; those below the horizontal line give the Standard Model calculated value as a function of the five parameters. Theory uncertainties are future projections assuming complete 3-loop calculations, based on estimates in Refs. [25, 26, 29, 30].

The inputs to the fit are listed in Table 1.7. Notice that we have performed the fit directly using forward-backward asymmetry parameters $A_{\text{FB}}^{0,f}$ as inputs, rather than the derived quantities $\sin^2 \theta_{\text{eff}}^f$ that were used in earlier work [31, 32]. The forward-backward asymmetries more directly reflect the experimental measurements; on the other hand, theoretical predictions are often expressed in terms of the effective weak mixing angles [26, 27]. They are related through the asymmetry parameters A_f :

$$A_f = \frac{1 - 4|Q_f| \sin^2 \theta_{\text{eff}}^f}{1 - 4|Q_f| \sin^2 \theta_{\text{eff}}^f + 8|Q_f|^2 \sin^4 \theta_{\text{eff}}^f}, \quad (1.4)$$

$$A_{\text{FB}}^{0,f} = \frac{3}{4} A_e A_f. \quad (1.5)$$

There is an extensive literature on the computation of the S and T dependence of observables (e.g. [17, 18, 33]); a convenient tabulation of the results may be found in Appendix A of [34]. Assembling these results, we obtain a prediction of the observables in terms of the five input parameters, S , and T . In the fit we compute a profile likelihood, floating the five parameters to obtain the maximum likelihood for given S and T .

The fit is performed following [31] (which in turn relied on [35–37]): in constructing a likelihood we treat experimental uncertainties as Gaussian but theory uncertainties as a flat prior, leading to an effective χ^2 function

$$\chi_{\text{mod}}^2 = \sum_j \left[-2 \log \left(\text{erf} \left(\frac{M_j - O_j + \delta_j}{\sqrt{2}\sigma_j} \right) - \text{erf} \left(\frac{M_j - O_j - \delta_j}{\sqrt{2}\sigma_j} \right) \right) - 2 \log \left(\sqrt{2\pi}\sigma_j \right) \right], \quad (1.6)$$

with M_j the measured value, O_j the prediction for the observable, σ_j the experimental uncertainty, and δ_j the theory uncertainty.

Our estimates of theory uncertainties assume that full three-loop computations of the parametric dependence of observables in the Standard Model will be completed. The remaining uncertainties are estimated based on [25, 26, 29, 30]. In the case of the W mass measurement, an uncertainty of 1 MeV from the computation of the near-threshold WW cross section is added in quadrature with the estimated four-loop theory uncertainty in the observable itself.

The results of the fit are depicted in Fig. 1.3. Solid contours are 68% confidence level curves, meaning $\Delta\chi_{\text{mod}}^2 = 2.30$; the dashed contour is 98% C.L. ($\Delta\chi_{\text{mod}}^2 = 6.18$). For clarity we have assumed that the measured central values will precisely agree with Standard Model predictions. In particular, the contour depicting current constraints is artificially displaced to be centered at the origin, though it accurately reflects the size of the uncertainties in current data. From the figure, we see that the results of CEPC will significantly shrink the error bars on the S and T parameters relative to currently available data.

By fixing $T = 0$ or $S = 0$, we can also obtain the projected one-parameter 68% C.L. bounds on S and T . As one-parameter fits these correspond to $\Delta\chi_{\text{mod}}^2 = 1.0$. We obtain:

$$|S| < 3.6 \times 10^{-2} \text{ (current)}, \quad 7.9 \times 10^{-3} \text{ (CEPC projection)}, \quad (1.7)$$

$$|T| < 3.1 \times 10^{-2} \text{ (current)}, \quad 8.4 \times 10^{-3} \text{ (CEPC projection)}. \quad (1.8)$$

Thus CEPC will achieve about a factor of 4 additional precision on both of the electroweak oblique parameters.

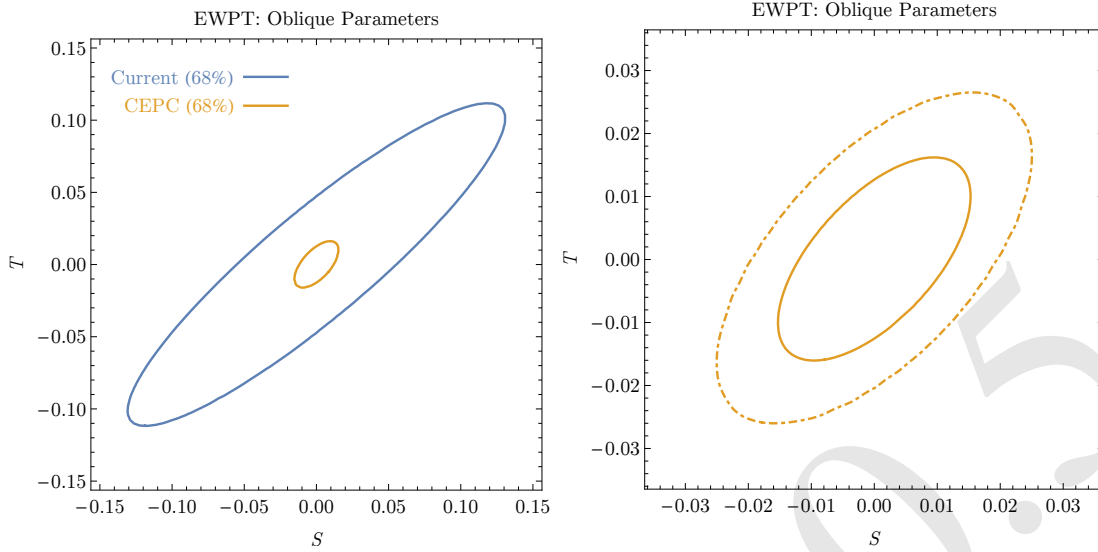


Figure 1.3: CEPC constraints on the oblique parameters S and T . Left panel: comparison of CEPC projection (orange) to current constraints (blue). Contours are 68% confidence level. Right panel: a closer look at the CEPC fit, showing 68% confidence level (solid) and 95% confidence level (dashed).

References

- [1] J. Erler, S. Heinemeyer, W. Hollik, G. Weiglein, and P. Zerwas, *Physics impact of GigaZ*, *Phys.Lett.* **B486** (2000) 125–133, [arXiv:hep-ph/0005024 \[hep-ph\]](#).
- [2] ALEPH Collaboration, DELPHI Collaboration, L3 Collaboration, OPAL Collaboration, LEP Electroweak Working Group Collaboration, J. Alcaraz et al., *A Combination of preliminary electroweak measurements and constraints on the standard model*, [arXiv:hep-ex/0612034 \[hep-ex\]](#).
- [3] L3 Collaboration, M. Acciarri et al., *Measurement of $R(b)$ and $Br(b \rightarrow \text{lepton neutrino } X)$ at LEP using double tag methods*, *Eur. Phys. J.* **C13** (2000) 47–61, [arXiv:hep-ex/9909045 \[hep-ex\]](#).
- [4] OPAL Collaboration, G. Abbiendi et al., *A Measurement of $R(b)$ using a double tagging method*, *Eur. Phys. J.* **C8** (1999) 217–239, [arXiv:hep-ex/9810002 \[hep-ex\]](#).
- [5] DELPHI Collaboration, P. Abreu et al., *A Precise measurement of the partial decay width ratio $R_b^0 = \Gamma(b\bar{b})/\Gamma(\text{had})$* , *Eur.Phys.J.* **C10** (1999) 415–442.
- [6] ALEPH Collaboration, R. Barate et al., *A Measurement of $R(b)$ using mutually exclusive tags*, *Phys. Lett.* **B401** (1997) 163–175.
- [7] SLD Collaboration, K. Abe et al., *Measurement of the branching ratio of the Z^0 into heavy quarks*, *Phys.Rev.* **D71** (2005) 112004, [arXiv:hep-ex/0503005 \[hep-ex\]](#).
- [8] OPAL Collaboration, G. Abbiendi et al., *Precise determination of the Z resonance parameters at LEP: 'Zedometry'*, *Eur. Phys. J.* **C19** (2001) 587–651, [arXiv:hep-ex/0012018 \[hep-ex\]](#).

- [9] DELPHI Collaboration, P. Abreu et al., *Cross-sections and leptonic forward backward asymmetries from the Z0 running of LEP*, *Eur. Phys. J.* **C16** (2000) 371–405.
- [10] L3 Collaboration, M. Acciarri et al., *Measurements of cross-sections and forward backward asymmetries at the Z resonance and determination of electroweak parameters*, *Eur. Phys. J.* **C16** (2000) 1–40, [arXiv:hep-ex/0002046](https://arxiv.org/abs/hep-ex/0002046) [hep-ex].
- [11] ALEPH Collaboration, R. Barate et al., *Measurement of the Z resonance parameters at LEP*, *Eur. Phys. J.* **C14** (2000) 1–50.
- [12] SLD Collaboration, K. Abe et al., *Direct measurements of A(b) and A(c) using vertex/kaon charge tags at SLD*, *Phys. Rev. Lett.* **94** (2005) 091801, [arXiv:hep-ex/0410042](https://arxiv.org/abs/hep-ex/0410042) [hep-ex].
- [13] ALEPH Collaboration Collaboration, A. Heister et al., *Measurement of A^b(FB) using inclusive b hadron decays*, *Eur.Phys.J.* **C22** (2001) 201–215, [arXiv:hep-ex/0107033](https://arxiv.org/abs/hep-ex/0107033) [hep-ex].
- [14] OPAL Collaboration Collaboration, G. Abbiendi et al., *Measurement of the b quark forward backward asymmetry around the Z0 peak using an inclusive tag*, *Phys.Lett.* **B546** (2002) 29–47, [arXiv:hep-ex/0209076](https://arxiv.org/abs/hep-ex/0209076) [hep-ex].
- [15] DELPHI Collaboration Collaboration, J. Abdallah et al., *Determination of A^b(FB) at the Z pole using inclusive charge reconstruction and lifetime tagging*, *Eur.Phys.J.* **C40** (2005) 1–25, [arXiv:hep-ex/0412004](https://arxiv.org/abs/hep-ex/0412004) [hep-ex].
- [16] L3 Collaboration Collaboration, M. Acciarri et al., *Measurement of the e⁺e⁻ → Z → b \bar{b} forward-backward asymmetry and the B0 anti-B0 mixing parameter using prompt leptons*, *Phys.Lett.* **B448** (1999) 152–162.
- [17] M. E. Peskin and T. Takeuchi, *A New constraint on a strongly interacting Higgs sector*, *Phys.Rev.Lett.* **65** (1990) 964–967.
- [18] M. E. Peskin and T. Takeuchi, *Estimation of oblique electroweak corrections*, *Phys.Rev.* **D46** (1992) 381–409.
- [19] J. Wudka, *Effective Lagrangians (for electroweak physics)*, in *4th Mexican Workshop on Particles and Fields Yucatan, Mexico, October 25-29, 1993*, pp. 61–106. 1994. [arXiv:hep-ph/9405206](https://arxiv.org/abs/hep-ph/9405206) [hep-ph].
- [20] J. Erler and F. Ayres, *Electroweak Model and Constraints on New Physics*, Particle Data Group review . <http://pdg.lbl.gov/2014/reviews/rpp2014-rev-standard-model.pdf>.
- [21] G. P. Lepage, P. B. Mackenzie, and M. E. Peskin, *Expected Precision of Higgs Boson Partial Widths within the Standard Model*, [arXiv:1404.0319](https://arxiv.org/abs/1404.0319) [hep-ph].
- [22] M. Baak, J. Cuth, J. Haller, A. Hoecker, R. Kogler, et al., *The global electroweak fit at NNLO and prospects for the LHC and ILC*, [arXiv:1407.3792](https://arxiv.org/abs/1407.3792) [hep-ph].

- [23] CMS Collaboration, *Projected improvement of the accuracy of top-quark mass measurements at the upgraded LHC*, CMS-PAS-FTR-13-017, CERN, Geneva, 2013. <https://cds.cern.ch/record/1605627>.
- [24] J. Erler, *Status of Precision Extractions of α_s and Heavy Quark Masses*, *AIP Conf. Proc.* **1701** (2016) 020009, [arXiv:1412.4435](https://arxiv.org/abs/1412.4435) [hep-ph].
- [25] M. Awramik, M. Czakon, A. Freitas, and G. Weiglein, *Precise prediction for the W boson mass in the standard model*, *Phys.Rev.* **D69** (2004) 053006, [arXiv:hep-ph/0311148](https://arxiv.org/abs/hep-ph/0311148) [hep-ph].
- [26] M. Awramik, M. Czakon, and A. Freitas, *Electroweak two-loop corrections to the effective weak mixing angle*, *JHEP* **0611** (2006) 048, [arXiv:hep-ph/0608099](https://arxiv.org/abs/hep-ph/0608099) [hep-ph].
- [27] I. Dubovyk, A. Freitas, J. Gluza, T. Riemann, and J. Usovitsch, *The two-loop electroweak bosonic corrections to $\sin^2 \theta_{\text{eff}}^b$* , *Phys. Lett.* **B762** (2016) 184–189, [arXiv:1607.08375](https://arxiv.org/abs/1607.08375) [hep-ph].
- [28] I. Dubovyk, A. Freitas, J. Gluza, T. Riemann, and J. Usovitsch, *Complete electroweak two-loop corrections to Z boson production and decay*, [arXiv:1804.10236](https://arxiv.org/abs/1804.10236) [hep-ph].
- [29] A. Freitas, K. Hagiwara, S. Heinemeyer, P. Langacker, K. Moenig, M. Tanabashi, and G. W. Wilson, *Exploring Quantum Physics at the ILC*, in *Proceedings, 2013 Community Summer Study on the Future of U.S. Particle Physics: Snowmass on the Mississippi (CSS2013): Minneapolis, MN, USA, July 29-August 6, 2013*. 2013. [arXiv:1307.3962](https://arxiv.org/abs/1307.3962) [hep-ph]. <https://inspirehep.net/record/1242667/files/arXiv:1307.3962.pdf>.
- [30] A. Freitas, *Higher-order electroweak corrections to the partial widths and branching ratios of the Z boson*, *JHEP* **04** (2014) 070, [arXiv:1401.2447](https://arxiv.org/abs/1401.2447) [hep-ph].
- [31] J. Fan, M. Reece, and L.-T. Wang, *Possible Futures of Electroweak Precision: ILC, FCC-ee, and CEPC*, [arXiv:1411.1054](https://arxiv.org/abs/1411.1054) [hep-ph].
- [32] C.-S. S. Group, *CEPC-SPPC Preliminary Conceptual Design Report. 1. Physics and Detector*, .
- [33] C. Burgess, S. Godfrey, H. Konig, D. London, and I. Maksymyk, *Model independent global constraints on new physics*, *Phys.Rev.* **D49** (1994) 6115–6147, [arXiv:hep-ph/9312291](https://arxiv.org/abs/hep-ph/9312291) [hep-ph].
- [34] M. Ciuchini, E. Franco, S. Mishima, and L. Silvestrini, *Electroweak Precision Observables, New Physics and the Nature of a 126 GeV Higgs Boson*, *JHEP* **1308** (2013) 106, [arXiv:1306.4644](https://arxiv.org/abs/1306.4644) [hep-ph].
- [35] A. Hocker, H. Lacker, S. Laplace, and F. Le Diberder, *A New approach to a global fit of the CKM matrix*, *Eur.Phys.J.* **C21** (2001) 225–259, [arXiv:hep-ph/0104062](https://arxiv.org/abs/hep-ph/0104062) [hep-ph].

Draft: Tuesday 7th August, 2018-10:58

- [36] H. Flacher, M. Goebel, J. Haller, A. Hocker, K. Monig, et al., *Revisiting the Global Electroweak Fit of the Standard Model and Beyond with Gfitter*, *Eur.Phys.J.* **C60** (2009) 543–583, [arXiv:0811.0009](#) [hep-ph].
- [37] R. Lafaye, T. Plehn, M. Rauch, D. Zerwas, and M. Duhrssen, *Measuring the Higgs Sector*, *JHEP* **0908** (2009) 009, [arXiv:0904.3866](#) [hep-ph].

Draft-V0.5